Journal of Computational Mathematics, Vol.26, No.3, 2008, 456–470.

ON THE P1 POWELL-SABIN DIVERGENCE-FREE FINITE ELEMENT FOR THE STOKES EQUATIONS*

Shangyou Zhang
Department of Mathematical Sciences, University of Delaware, DE 19716, USA
Email: szhang@udel.edu

Dedicated to Professor Junzhi Cui on the occasion of his 70th birthday

Abstract

The stability of the P_1-P_0 mixed-element is established on general Powell-Sabin triangular grids. The piecewise linear finite element solution approximating the velocity is divergence-free pointwise for the Stokes equations. The finite element solution approximating the pressure in the Stokes equations can be obtained as a byproduct if an iterative method is adopted for solving the discrete linear system of equations. Numerical tests are presented confirming the theory on the stability and the optimal order of convergence for the P_1 Powell-Sabin divergence-free finite element method.

Mathematics subject classification: 65M60, 65N30, 76D07.
Key words: Powell Sabin triangles, Mixed finite elements, Stokes, Divergence-free element.

1. Introduction

A natural finite element method for the Stokes equations would be the P_k-P_{k-1} mixed element which approximates the velocity by continuous P_k piecewise-polynomials and approximates the pressure by discontinuous P_{k-1} piecewise-polynomials. One advantage of the element is to preserve the incompressibility condition of incompressible fluids, i.e., the discrete velocity is also divergence-free pointwise [2, 3, 18, 28, 29, 34]. Another advantage is its simplicity in computation that the mixed element can be reduced to the standard C_0 finite element solving Laplace equations, as the discrete pressure is a byproduct when an iterative method is used for the linear system of discrete equations. A fundamental study on the method was done by Scott and Vogelius in 1983 [28, 29] that the method is stable and consequently of the optimal order on 2D triangular grids for any $k \geq 4$, provided that the grids have no nearly-singular vertex (a vertex is called singular if all edges meeting at the vertex form two cross lines.) For $k \leq 3$, Scott and Vogelius showed the method would not be stable for general triangular grids, in [28, 29]. Nevertheless, for low order elements, ($k < 4$), the P_k-P_{k-1} element can still be stable if the underlying triangulations are of certain types. The stability is shown for the Hsieh-Clough-Tocher triangles with $k \geq 2$ [24], for the quadrilateral-triangulations with $k = 2$ [2], for the uniform criss-cross grids with $k = 1$ [25] and for the 3D Hsieh-Clough-Tocher tetrahedral grids with $k \geq 3$ [35].

To establish the convergence of the finite element solution for the pressure, a uniform (independent of the grid size h) inf-sup condition, (cf. (3.7)), known as LBB condition (cf. [6]), is usually required. For example, when a nearly-singular vertex approaches to singular (cf.

* Received February 14, 2008 / accepted March 3, 2008 /

[28, 29]), the inf-sup constant approaches to zero for the mixed element space P_k-P_{k-1}. Nevertheless, when the vertex becomes a singular one, the inf-sup constant would jump back from zero to a regular one, because the extra spurious pressure mode is filtered out automatically in the divergence-free element method. This is exactly the situation for the P_1-P_0 mixed element on Powell-Sabin grids. To be precise, here the discrete space for the pressure is the divergence of C_0-P_1 conforming element space, a proper subspace of the C_{-1}-P_0 space on the grid. Via the macro-element technique [6, 31] and a local L^2-orthogonal decomposition (see (3.14) below), we prove the inf-sup condition for the P_1-P_0 mixed element on Powell-Sabin grids. The stability of this P_1 Powell-Sabin element has not been fully studied previously, but the element was used in computation, cf. [8]. We note that the name of divergence-free mixed element is used often for non-conforming [4, 21, 32] or discontinuous Galerkin methods [7, 10, 14, 17], or even for weakly divergence-free methods [33]. But here, the discrete solutions for the velocity are truly divergence-free, including the points on the inter-element boundary.

The rest of the paper is divided into the following sections. In Section 2, we define the divergence-free finite element method and prove the uniqueness of such finite element solution. We will show how to reduce the P_k-P_{k-1} mixed element to the C_0-P_k element, and how to apply the classic iterated penalty method to solve the discrete, but positive definite, linear systems of equations. In Section 3, we will show the inf-sup condition for the Powell-Sabin element. In Section 4 we provide numerical tests using the Powell-Sabin P_1 divergence-free element.

2. The Divergence-free Finite Element

In this section, we shall define the divergence-free finite elements for the stationary Stokes equations. The resulting linear systems of equations, by such elements, are shown to have a unique solution. The classic iterated penalty method is introduced, which solves the discrete linear system and generates the discrete pressure solution as a byproduct.

We consider the stationary Stokes equations: Find functions $\mathbf{u}$ (the fluid velocity) and p (the pressure) on a 2D polygonal domain $\Omega \subset \mathbf{R}^2$ such that

$$\begin{aligned} -\Delta \mathbf{u} + \nabla p &= \mathbf{f} && \text{in } \Omega, \\ \operatorname{div} \mathbf{u} &= 0 && \text{in } \Omega, \\ \mathbf{u} &= \mathbf{0} && \text{on } \partial\Omega, \end{aligned} \tag{2.1}$$

where $\mathbf{f}$ is the body force. Via the integration by parts, we get a variational problem for the Stokes equations: Find $\mathbf{u} \in H_0^1(\Omega)^2$ and $p \in L_0^2(\Omega) := L^2(\Omega)/C = \{p \in L^2 \mid \int_\Omega p = 0\}$ such that

$$\begin{aligned} a(\mathbf{u}, \mathbf{v}) + b(\mathbf{v}, p) &= (\mathbf{f}, \mathbf{v}) && \forall \mathbf{v} \in H_0^1(\Omega)^2, \\ b(\mathbf{u}, q) &= 0 && \forall q \in L_0^2(\Omega). \end{aligned} \tag{2.2}$$

Here $H_0^1(\Omega)^2$ is the subspace of the Sobolev space $H^1(\Omega)^2$ (cf. [9]) with zero boundary trace, and

$$\begin{aligned} a(\mathbf{u}, \mathbf{v}) &= \int_\Omega \nabla \mathbf{u} \cdot \nabla \mathbf{v} \, dx, \\ b(\mathbf{v}, p) &= -\int_\Omega \operatorname{div} \mathbf{u} \, p \, dx, \\ (\mathbf{f}, \mathbf{v}) &= \int_\Omega \mathbf{f} \, \mathbf{v} \, dx. \end{aligned}$$

Let Ω be quasi-uniformly triangulated [9]:

$$\Omega_h = \{T \mid T \text{ is a triangle with the minimum angle bounded, } |T| \le h\}. \tag{2.3}$$

Let $\mathbf{V}_h$ be the space of continuous piecewise polynomial of degree k on Ω with the homogeneous boundary condition:

$$\mathbf{V}_h = \left\{\mathbf{u}_h \in C(\Omega) \mid \mathbf{u}_h|_T \in P_k(T)^2 \ \forall T \in \Omega_h, \text{ and } \ \mathbf{u}_h|_{\partial\Omega} = 0\right\}. \tag{2.4}$$

Then we define

$$P_h = \{\operatorname{div} \mathbf{u}_h \mid \mathbf{u}_h \in \mathbf{V}_h\}. \tag{2.5}$$

Since $\int_\Omega p_h = \int_\Omega \operatorname{div} \mathbf{u}_h = \int_{\partial\Omega} \mathbf{u}_h \cdot \mathbf{n} = 0$ for any $p_h \in P_h$, we conclude that

$$\mathbf{V}_h \subset H_0^1(\Omega)^2, \quad P_h \subset L_0^2(\Omega),$$

i.e., the mixed-finite element pair $(\mathbf{V}_h, P_h)$ is conforming.

Then the finite element discretization of problem (2.2) reads: Find $\mathbf{u}_h \in \mathbf{V}_h$ and $p_h \in P_h$ such that

$$\begin{aligned} &a(\mathbf{u}_h, \mathbf{v}) + b(\mathbf{v}, p_h) = (\mathbf{f}, \mathbf{v}) \quad && \forall \mathbf{v} \in \mathbf{V}_h, \\ &b(\mathbf{u}_h, q) = 0 && \forall q \in P_h. \end{aligned} \tag{2.6}$$

We note that by (2.5), P_h is a subspace of discontinuous, piecewise polynomials of degree $(k-1)$ or less. Except a few cases such as the high-order tetrahedral elements on Hsieh-Clough-Tocher grids (cf. [34]), P_h does not include all mean-value zero piecewise polynomials of degree $(k-1)$. So it is not possible to find a local basis for P_h in general, and it is not possible to derive a linear system of equations for (2.6), different from all other mixed finite methods. It seems that the definition of P_h (2.5) is not practical to implement the mixed element. But on the other side, it is the special interest of the new formulation where the space P_h is not implemented at all, and the discrete solutions approximating the pressure function in the Stokes equations will be obtained as byproducts. So there will be only one finite element space for the velocity, and the mixed element pair becomes a single element. This does not only greatly simplify the coding work, but also avoids the difficulty of solving non-positive definite systems of linear equations encountered in the classic mixed element method.

Let us introduce a key finite element space, the divergence-free finite element space,

$$\mathbf{Z}_h = \{\mathbf{u}_h \in \mathbf{V}_h \mid \operatorname{div} \mathbf{u}_h = 0\}. \tag{2.7}$$

Because of the special definition (2.5) of P_h, the solution $\mathbf{u}_h$ of (2.6) is always divergence-free pointwise, i.e., $\mathbf{u}_h \in \mathbf{Z}_h$, shown below.

Proposition 2.1. *Let $\mathbf{V}_h$ be defined by* (2.4) *on any 2D triangulation, with or without singular or nearly singular vertices, of quasi-uniform or graded grids, of regular or degenerating grids, and for any degree of polynomial $k \ge 1$. Let P_h be defined by* (2.5). *The discrete linear system* (2.6) *has a unique solution:*

$$\mathbf{u}_h \in \mathbf{Z}_h, \quad p_h \in P_h.$$

Proof. We show the uniqueness first. Let $\mathbf{u}_h$ be a solution of (2.6). We have, by the second equation,

$$b(\mathbf{u}_h, q) = 0 \ \Rightarrow \ \int_\Omega \operatorname{div} \mathbf{u}_h \operatorname{div} \mathbf{u}_h = 0 \ \Rightarrow \ \mathbf{u}_h \in \mathbf{Z}_h,$$

where we have chosen $q = \operatorname{div} \mathbf{u}_h \in P_h$. Now, if $\tilde{\mathbf{u}}_h$ is another solution of (2.6), by the first equation, because $\operatorname{div} \tilde{\mathbf{u}}_h = 0$ as shown above, we get

$$a(\mathbf{u}_h - \tilde{\mathbf{u}}_h, \mathbf{u}_h - \tilde{\mathbf{u}}_h) = 0,$$

where we have chosen $\mathbf{v} = \mathbf{u}_h - \tilde{\mathbf{u}}_h$ so that the term involving two pressure solutions drops as $\operatorname{div} \mathbf{v} = 0$. Therefore we have shown $\mathbf{u}_h$ is unique (if it does exist.)

Next, let $(\mathbf{u}_h, p_h)$ and $(\mathbf{u}_h, \tilde{p}_h)$ be two solutions of (2.6). It follows that

$$b(\mathbf{v}, p_h - \tilde{p}_h) = 0 \ \Rightarrow \int_\Omega (p_h - \tilde{p}_h)^2 = 0,$$

where we have chosen one $\mathbf{v}$ so that $\operatorname{div} \mathbf{v} = p_h - \tilde{p}_h$, by the definition (2.5). So we conclude the solution p_h is unique too.

Finally, because (2.6) is a linear system of finitely many equations, the uniqueness implies the existence. □

We remark that an inf-sup condition is required to ensure the existence of solution for general mixed finite elements. Therefore, for divergence-free finite elements, the inf-sup condition always holds, except that the inf-sup constant in the inequality may depend on the grid, i.e., it may be very close to zero sometimes.

Proposition 2.1 ensures the finite element system (2.6) has a unique solution. We introduce a classic iterated penalty method to find the unique solution. We will show how to reduce the mix-element space to a single element space in the method. The method is an iterative one for solving conforming P_k element Laplace equations, in essence.

Definition 2.1. (*The iterated penalty method for the divergence-free element.* [5, 6, 11, 13, 30]) *Let the initial iterate* $\mathbf{u}_h^0 = \mathbf{0}$ *for the finite element Stokes equation* (2.6). *The rest iterates* $\mathbf{u}_h^n$ *are defined sequentially as the unique solution of*

$$a(\mathbf{u}_h^n, \mathbf{v}_h) + \alpha(\operatorname{div} \mathbf{u}_h^n, \operatorname{div} \mathbf{v}_h) = (\mathbf{f}, \mathbf{v}_h) + \beta(\operatorname{div} \sum_{j=0}^{n-1} \mathbf{u}_h^j, \operatorname{div} \mathbf{v}_h) \quad \forall \mathbf{v}_h \in \mathbf{V}_h, \tag{2.8}$$

$n = 1, 2, \cdots$. *Here* α *and* β *are positive constants. At the end of iteration, we let*

$$p_h^n = \beta \operatorname{div} \sum_{j=0}^{n} \mathbf{u}_h^j. \tag{2.9}$$

Remark 2.1. In the iterated penalty method of Definition 2.1, we need only to do computer coding for the conforming C_0-P_k element for the vector Laplacian like equations. This avoids a heavy work for coding the discontinuous finite elements for the pressure.

Remark 2.2. The convergence speed of the iterated penalty method in Definition 2.1 is shown to be constant, independent of the grid size h, in [5] under the inf-sup condition.

Remark 2.3. The iterated penalty method of Definition 2.1 can be a nested-iteration method. As usual, the inner equation would be solved by another iterative method, for example, the multigrid iteration [30], up to a certain accuracy. In other words, the inner iteration and the outer iteration would be combined into one.

To conclude this section, we show a lemma about the equivalence, in fact, an identity, of the semi H^1-inner product and the div + curl product, for C_0-P_k polynomials. This is well known. But we could not find a rigorous proof anywhere, as it seems that the differentiability is assumed.

Lemma 2.1. *For all $\mathbf{u}, \mathbf{v} \in \mathbf{V}_h$, in both 2D and 3D, it holds that*

$$a(\mathbf{u}, \mathbf{v}) = (\operatorname{div} \mathbf{u}, \operatorname{div} \mathbf{v}) + (\operatorname{curl} \mathbf{u}, \operatorname{curl} \mathbf{v}). \tag{2.10}$$

Proof. We note that $\operatorname{curl} \mathbf{u}$ is a scalar function in 2D, but a vector function in 3D, $\mathbf{curl}\, \mathbf{u}$. We will show (2.10) in 2D first. Let $\mathbf{u} = \langle u_1, u_2 \rangle$, $\mathbf{v} = \langle v_1, v_2 \rangle$, and $\mathbf{x} = \langle x, y \rangle$.

$$\begin{aligned}
a(\mathbf{u}, \mathbf{v}) &= \sum_{T \in \Omega_h} \int_T (u_{1x} v_{1x} + u_{1y} v_{1y} + u_{2x} v_{2x} + u_{2y} v_{2y}) d\mathbf{x}, \\
(\operatorname{div} \mathbf{u}, \operatorname{div} \mathbf{v}) &= \sum_{T \in \Omega_h} \int_T (u_{1x} v_{1x} + u_{1x} v_{2y} + u_{2y} v_{1x} + u_{2y} v_{2y}) d\mathbf{x}, \\
(\operatorname{curl} \mathbf{u}, \operatorname{curl} \mathbf{v}) &= \sum_{T \in \Omega_h} \int_T (u_{2x} v_{2x} - u_{2x} v_{1y} - u_{1y} v_{2x} + u_{1y} v_{1y}) d\mathbf{x}.
\end{aligned}$$

We need to show the cancellation of 4 terms in the middle of $(\operatorname{div} \mathbf{u}, \operatorname{div} \mathbf{v})$ and $(\operatorname{curl} \mathbf{u}, \operatorname{curl} \mathbf{v})$. This is done by the integration by parts.

$$\begin{aligned}
\int_T u_{1x} v_{2y} dy dx &= \int_T (u_1 v_{2y})_x dy dx - \int_T u_1 v_{2yx} dy dx \\
&= \int_{\partial T} u_1 v_{2y} dy - \Big(\int_T (u_1 v_{2x})_y dy dx - \int_T u_{1y} v_{2x} dy dx \Big) \\
&= \int_{\partial T} u_1 v_{2y} dy - \int_{\partial T} u_1 v_{2x} dx + \int_T u_{1y} v_{2x} dy dx \\
&= \int_{\partial T} u_1 \frac{\partial v_2}{\partial \mathbf{t}} ds + \int_T u_{1y} v_{2x} dy dx.
\end{aligned}$$

We note that the normal derivative $\partial v_2 / \partial \mathbf{n}$ is not continuous across two elements, but the tangential derivative $\partial v_2 / \partial \mathbf{t}$ is. When summing above integrals on all triangles, as u_1 is continuous on internal edges, the two integrals on the two sides of each internal edge are canceled. In addition, u_1 is zero at the boundary of Ω. So it follows that

$$\int_\Omega u_{1x} v_{2y} d\mathbf{x} - \int_\Omega u_{1y} v_{2x} d\mathbf{x} = 0.$$

Similarly we can do such an integration by parts for the other pair of terms. Hence (2.10) holds in 2D.

We now study the 3D case. The terms inside the integral over a tetrahedron T for $a(\mathbf{u}, \mathbf{v})$, for $(\operatorname{div} \mathbf{u}, \operatorname{div} \mathbf{v})$, and for $(\mathbf{curl}\, \mathbf{u}, \mathbf{curl}\, \mathbf{v})$, are, respectively,

$$\begin{aligned}
&u_{1x} v_{1x} + u_{1y} v_{1y} + u_{1z} v_{1z} + u_{2x} v_{2x} + u_{2y} v_{2y} + u_{2z} v_{2z} + u_{3x} v_{3x} + u_{3y} v_{3y} + u_{3z} v_{3z}, \\
&u_{1x} v_{1x} + u_{1x} v_{2y} + u_{1x} v_{3z} + u_{2y} v_{1x} + u_{2y} v_{2y} + u_{2y} v_{3z} + u_{3z} v_{1x} + u_{3z} v_{2y} + u_{3z} v_{3z}, \\
&u_{2x} v_{2x} - u_{2x} v_{1y} - u_{1y} v_{2x} + u_{1y} v_{1y} \quad + u_{1z} v_{1z} - u_{1z} v_{3x} - u_{3x} v_{1z} + u_{3x} v_{3x} \\
&\qquad + u_{3y} v_{3y} - u_{3y} v_{2z} - u_{2z} v_{3y} + u_{2z} v_{2z}.
\end{aligned}$$

Thus what we need to show is that

$$\int_\Omega (u_{1x}v_{2y} + u_{1x}v_{3z} + u_{2y}v_{1x} + u_{2y}v_{3z} + u_{3z}v_{1x} + u_{3z}v_{2y} \\ -u_{1y}v_{2x} - u_{1z}v_{3x} - u_{2x}v_{1y} - u_{2z}v_{3y} - u_{3x}v_{1z} - u_{3y}v_{2z})\, d\mathbf{x} = 0. \tag{2.11}$$

We study one pair of such terms on one tetrahedron $T \in \Omega_h$, by the divergence theorem, as follows.

$$\int_T (u_{1x}v_{2y} - u_{1y}v_{2x}) d\mathbf{x} = \int_{\partial T} (u_1 v_{2y} n_x - u_1 v_{2x} n_y + 0) dS \\ = \int_{\partial T} u_1 (\mathbf{n} \times \nabla v_2)_3 dS.$$

Here we denote the normal vector on the triangular faces of T by $\mathbf{n} = \langle n_x, n_y, n_z \rangle$. We note that all three components of "tangential derivatives"

$$\mathbf{n} \times \nabla v_2 = \langle (\mathbf{n} \times \nabla v_2)_1, (\mathbf{n} \times \nabla v_2)_2, (\mathbf{n} \times \nabla v_2)_3 \rangle$$

are continuous at the inter element boundaries and are zero at the domain boundary. Therefore (2.10) holds in 3D and the lemma is proven. □

3. The Powell-Sabin P1 Divergence-free Element

We will define the Powell-Sabin triangulation and the P_1 divergence-free element on such triangulations. We will establish the inf-sup condition for the Powell-Sabin P_1 divergence-free element, and consequently, the optimal order of convergence.

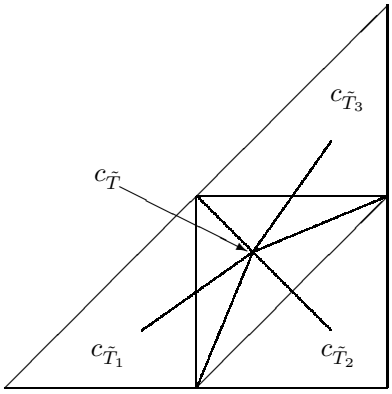

Fig. 3.1. A Powell-Sabin split of the central triangle $\tilde{T}$.

Let Ω be a 2D polygonal domain triangulated into a quasi-uniform grid $\tilde{\Omega}_h$ (c.f. (2.3), [5, 9]). For each triangle $\tilde{T} \in \tilde{\Omega}_h$, let $c_{\tilde{T}}$ be the center of the inscribed circle of $\tilde{T}$, see Fig. 3.1. To define the Powell-Sabin triangulation Ω_h based on $\tilde{\Omega}_h$, we connect each $c_{\tilde{T}}$ to both the three vertices of $\tilde{T}$ (this is the Hsieh-Clough-Tocher triangulation, cf. [1, 9, 16, 19, 24, 26, 27, 35] and Fig. 3.6) and the three $c_{\tilde{T}_i}$ of the three neighboring triangles $\tilde{T}_i$ in $\tilde{\Omega}_h$ (c.f. Fig. 3.1, [1, 16, 22, 23, 27]). If $\tilde{T}$ is a boundary triangle, we simply connect $c_{\tilde{T}}$ to the mid-point of the boundary edge(s).

In this fashion, each triangle of $\tilde{\Omega}_h$ splits into 6 subtriangles, see Fig. 3.2. We call the resulting triangulation a Powell-Sabin triangulation, Ω_h. It can be shown (see the references in [15]) that the family of Powell-Sabin triangulations derived from a quasi-uniform family triangulations is also quasi-uniform. We note also that the interior point on each triangle $\tilde{T}$ can be chosen differently, in general. However, we can see that by choosing the point $c_{\tilde{T}_i}$ to be the center of the inscribed circle of $\tilde{T}_i$, it is guaranteed that the intersection of the edge $c_{\tilde{T}_1}c_{\tilde{T}_2}$ and the common edge between triangles $\tilde{T}_1$ and $\tilde{T}_2$ is an interior point on the common edge. In fact, the intersection point is between the two projection points of $c_{\tilde{T}_1}$ and $c_{\tilde{T}_2}$ on the common edge. We remark that there is no restriction on $\tilde{\Omega}_h$ here. However, if we would like to have a nested multigrid-refinement of $\tilde{\Omega}_h$ and a nested family of Powell-Sabin finite element spaces, $\tilde{\Omega}_h$ would be no longer an arbitrary triangulation (see [20]). We note that the center of the inscribed circle is used in Fig. 3.1, but the center of mass is used in Fig. 3.2. In either case, computationally, we would assume that the initial grid $\tilde{\Omega}_h$ is quasiuniform and regular enough such that the center point is away from the boundary of the triangle and that the six subtriangles, T_j, $j = 1, \cdots, 6$, of $\tilde{T}$, are about the same size:

$$\text{distance}(c_{\tilde{T}}, \partial\tilde{T}) \geq Ch, \quad \text{area}(T_j) \geq Ch^2, \quad \text{for all } \tilde{T} \in \Omega_h, \tag{3.1}$$

for some $C > 0$ independent of h.

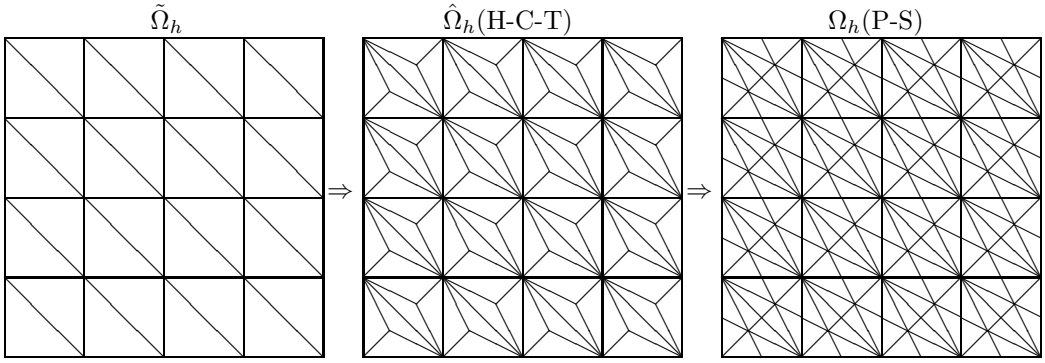

Fig. 3.2. A uniform triangulation $\tilde{\Omega}_h$ splits into a Powell-Sabin grid Ω_h.

To be clear, we use another notation for the Powell-Sabin C_0-P_1 space, different from the general space $\mathbf{V}_h$ in (2.4), on the grid Ω_h.

$$\mathbf{V}_h^{PS} = \{\mathbf{v} \mid v|_T \in P_1 \ \forall T \in \Omega_h\} \cap H_0^1(\Omega)^2. \tag{3.2}$$

To show the inf-sup condition for the Powell-Sabin mixed P_1-P_0 element, we introduce auxiliary spaces for the pressure in the Stokes equations. One is the piecewise-constant space on the base triangulation $\tilde{\Omega}_h$ of a Powell-Sabin triangulation:

$$\tilde{P}_h = \left\{\tilde{q}_h \in L_0^2(\Omega) \mid \tilde{q}_h|_{\tilde{T}} = \tilde{q}_{\tilde{T}}, \text{ a constant, on each triangle } \tilde{T} \in \tilde{\Omega}_h\right\}. \tag{3.3}$$

It is well known that the P_2-P_0 combination mixed element is uniformly stable. In fact, the P_2-P_0 pair and the P_1-P_0 pair on half-sized grids, cf. Fig. 3.3, are two mostly used tools in the macro-element technique for showing the stability of other mixed finite elements, cf. Stenberg [31] and Arnold & Qin [2]. For the pair $(\mathbf{V}_h^{PS}, \tilde{P}_h)$, we have more degrees of freedom for the velocity while having the same pressure space, compared with the P_2-P_0 element, cf.

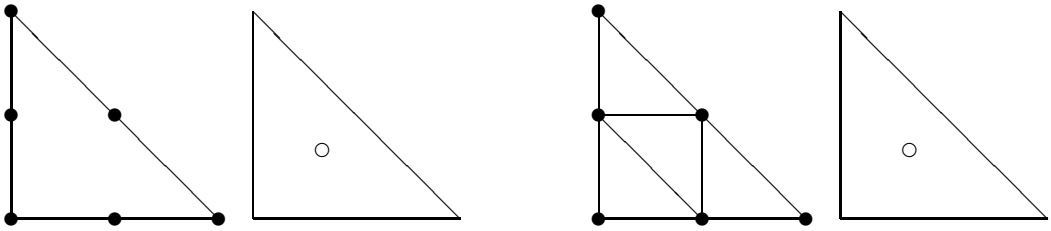

C_0–P_2 velocity, C_{-1}–P_0 pressure C_0–P_1 velocity on $\tilde{\Omega}_{\frac{h}{2}}$, C_{-1}–P_0 pressure on $\tilde{\Omega}_h$

Fig. 3.3. Two pairs of stable mixed finite elements.

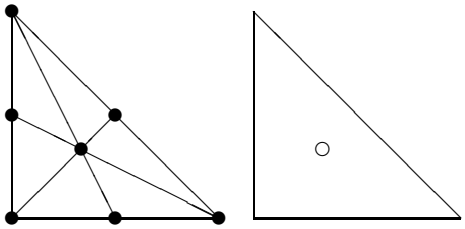

C_0–P_1 velocity on Ω_h, C_{-1}–P_0 pressure on $\tilde{\Omega}_h$

Fig. 3.4. A stable pair of mixed finite elements (Powell-Sabin grids for the velocity).

Figs. 3.3 and 3.4. Using the same analysis for the P_2-P_0 mixed element, cf. Stenberg [31], it is straightforward to show the pair $(\mathbf{V}_h^{PS}, \tilde{P}_h)$ is uniformly stable, as stated in the next lemma.

Lemma 3.1. *The mixed finite element pair* $(\mathbf{V}_h^{PS}, \tilde{P}_h)$*, defined in* (3.2) *and* (3.3)*, is uniformly stable, i.e., for some* C *independent of* h*,*

$$\inf_{\tilde{q}_h \in \tilde{P}_h} \sup_{\mathbf{v}_h \in \mathbf{V}_h^{PS}} \frac{b(\mathbf{v}_h, \tilde{q}_h)}{|\mathbf{v}_h|_{H^1} \|\tilde{q}_h\|_{L^2}} \geq C > 0. \tag{3.4}$$

We next enlarge the pressure space to get another auxiliary space. Instead of one constant each macro-triangle, we have three constants on each such a macro-triangle. Here, we split each triangle of $\tilde{\Omega}_h$ into three triangles, instead of six,

$$\hat{\Omega}_h = \{\hat{T}_i \mid \hat{T}_1 \cup \hat{T}_2 \cup \hat{T}_3 = \tilde{T} \in \tilde{\Omega}_h\},$$

shown in Figs. 3.2 and 3.5. Such a triangulation is called a Hsieh-Clough-Tocher grid, cf. Ciarlet [9] and Qin [24]. We define the second auxiliary space for the pressure on macro-grids $\hat{\Omega}_h$.

$$\hat{P}_h = \left\{ \hat{q}_h \in L_0^2(\Omega) \mid \hat{q}_h|_{\hat{T}} = \hat{q}_{\hat{T}}, \text{ a constant, on each triangle } \hat{T} \in \hat{\Omega}_h \right\}. \tag{3.5}$$

Lemma 3.2. *The mixed finite element pair* $(\mathbf{V}_h^{PS}, \hat{P}_h)$*, defined in* (3.2) *and* (3.5)*, is uniformly stable, i.e., for some positive* C *independent of* h*,*

$$\inf_{\hat{q}_h \in \hat{P}_h} \sup_{\mathbf{v}_h \in \mathbf{V}_h^{PS}} \frac{b(\mathbf{v}_h, \hat{q}_h)}{|\mathbf{v}_h|_{H^1} \|\hat{q}_h\|_{L^2}} \geq C. \tag{3.6}$$

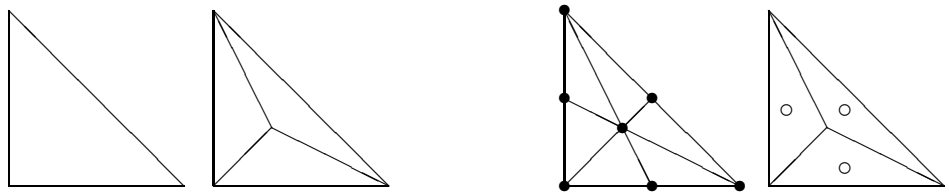

Fig. 3.5. A Hsieh-Clough-Tocher grid and a stable pair of mixed finite elements.

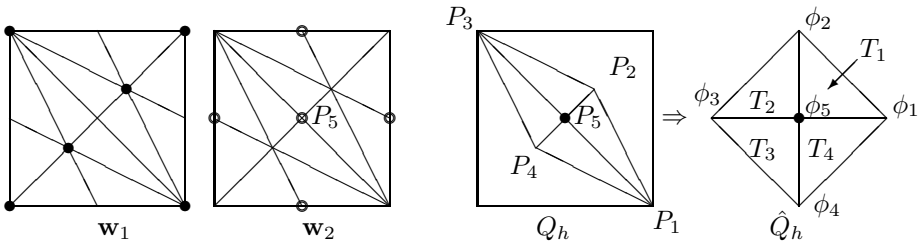

Fig. 3.6. A decomposition $\mathbf{w}_h = \mathbf{w}_1 + \mathbf{w}_2$, and a reference mapping.

Proof. The proof is done by the macro-element technique, similar to that for the inf-sup conditions on P_2-P_1 Hsieh-Clough-Tocher triangles, cf. [2] and [24], and on 3D P_3-P_2 Hsieh-Clough-Tocher tetrahedra [34]. We outline the proof. When restricted on a triangle $\tilde{T}$ of $\tilde{\Omega}_h$, the dimension of null space of the B-operator arising from $b(\cdot,\cdot)$ is 1, i.e.,

$$\dim N_{\tilde{T}} = \dim\{\hat{q}_h|_{\tilde{T}} \mid \hat{q}_h \in \hat{P}_h \text{ and } \ b(\mathbf{v}_h, \hat{q}_h) = 0 \ \forall \mathbf{v}_h \in \mathbf{V}_h^{PS}\} = 1 \quad \forall \tilde{T} \in \tilde{\Omega}_h.$$

We then apply the macro-element technique of Stenberg [31]. Here the key factor is the existence of a degree of freedom for $\mathbf{v}_h$ inside each edge of $\tilde{\Omega}_h$. (3.6) follows from (3.4). □

We will show next the stability of the Powell-Sabin divergence-free P_1 element, i.e., the space for the pressure is taken to be the divergence of the velocity space $\mathbf{V}_h^{PS}$, as defined in (2.5). Here the pressure spaces $\tilde{P}_h$ and $\hat{P}_h$ are extended further to P_h.

Theorem 3.1. *The mixed finite element pair* $(\mathbf{V}_h^{PS}, P_h)$*, defined in* (3.2) *and* (2.5)*, is uniformly stable on Powell-Sabin grids, i.e.,*

$$\inf_{q_h \in P_h} \sup_{\mathbf{v}_h \in \mathbf{V}_h^{PS}} \frac{b(\mathbf{v}_h, q_h)}{|\mathbf{v}_h|_{H^1} \|q_h\|_{L^2}} \geq C. \tag{3.7}$$

Proof. Let $q_h \in P_h$. Let $\mathbf{w}_h \in \mathbf{V}_h^{PS}$ be one such a function whose divergence is q_h: $\operatorname{div} \mathbf{w}_h = q_h$. To prove the inf-sup condition (3.4), we need to construct a $\mathbf{v}_h$ close to $\mathbf{w}_h$, filtering out the divergence-free component of $\mathbf{w}_h$. The construction of $\mathbf{v}_h$ is done in two steps. Let

$$\mathbf{w}_h = \mathbf{w}_1 \oplus \mathbf{w}_2, \quad \mathbf{w}_1 \in \mathbf{V}_1^{PS}, \ \mathbf{w}_2 \in \mathbf{V}_2^{PS}, \tag{3.8}$$

where $\mathbf{V}_1^{PS}$ is the C_0-P_1 subspace of $\mathbf{V}_h^{PS}$ on the Hsieh-Clough-Tocher grid $\hat{\Omega}_h$ (cf. Figs. 3.2, 3.5 and 3.6) and $\mathbf{V}_2^{PS}$ is the span of nodal basis functions of $\mathbf{V}_h^{PS}$ at the points interior to edges of $\tilde{\Omega}_h$, shown as P_5 in Fig. 3.6.

Without loss of generosity (by shifting Q_h to the origin), let $P_5(0,0)$ be a mid-edge point in the Powell-Sabin triangulation Ω_h. With the four neighbor points, cf. Fig. 3.6,

$$P_1(x_1, y_1), \ P_2(x_2, y_2), \ P_3(-cx_1, -cy_1), \ \text{ and } \ P_4(-dx_2, -dy_2),$$

the four triangles in Ω_h meeting at P_5 form a quadrilateral Q_h. Here c and d are two positive constants. If $c = 1/2$, P_5 would be the true middle point of edge P_1P_3. The referencing linear mapping for the first triangle $P_1P_2P_5$ is:

$$\begin{pmatrix} x \\ y \end{pmatrix} = \begin{pmatrix} x_1 & x_2 \\ y_1 & y_2 \end{pmatrix} \begin{pmatrix} \hat{x} \\ \hat{y} \end{pmatrix} =: B \begin{pmatrix} \hat{x} \\ \hat{y} \end{pmatrix}.$$

It leads to the standard finite element calculation of gradient vectors,

$$\nabla_{x,y} u \begin{pmatrix} x \\ y \end{pmatrix} = B^{-T} \nabla_{\hat{x},\hat{y}} \hat{u} \begin{pmatrix} \hat{x} \\ \hat{y} \end{pmatrix} = \frac{\begin{pmatrix} y_2 & -y_1 \\ -x_2 & x_1 \end{pmatrix}}{x_1 y_2 - x_2 y_1} \begin{pmatrix} u_1 - u_5 \\ u_2 - u_5 \end{pmatrix},$$

where u denotes a linear function and $u_i = u(P_i)$. The calculation is similar on the other three triangles. Let $\mathbf{v} = \begin{pmatrix} u & v \end{pmatrix}^T \in \mathbf{V}_h^{PS}$. Then $\operatorname{div} \mathbf{v}$ consists of four constants on the four triangles, see Fig. 3.6,

$$\begin{aligned}
\operatorname{div} \mathbf{v}|_{T_1} &= \hat{y}_2(u_1 - u_5) - \hat{y}_1(u_2 - u_5) - \hat{x}_2(v_1 - v_5) + \hat{x}_1(v_2 - v_5), \\
\operatorname{div} \mathbf{v}|_{T_2} &= \hat{y}_2 \frac{u_3 - u_5}{-c} - \hat{y}_1(u_2 - u_5) - \hat{x}_2 \frac{v_3 - v_5}{-c} + \hat{x}_1(v_2 - v_5), \\
\operatorname{div} \mathbf{v}|_{T_3} &= \hat{y}_2 \frac{u_3 - u_5}{-c} - \hat{y}_1 \frac{u_4 - u_5}{-d} - \hat{x}_2 \frac{v_3 - v_5}{-c} + \hat{x}_1 \frac{v_4 - v_5}{-d}, \\
\operatorname{div} \mathbf{v}|_{T_4} &= \hat{y}_2(u_3 - u_5) - \hat{y}_1 \frac{u_4 - u_5}{-d} - \hat{x}_2(v_3 - v_5) + \hat{x}_1 \frac{v_4 - v_5}{-d}.
\end{aligned} \tag{3.9}$$

The dimension of $\left(\operatorname{div} \mathbf{V}_h^{PS}\right)_{Q_h}$ can be easily found. It is 3, not 4, as P_5 is a singular-vertex. In fact, denoting the four constant values of $\operatorname{div} \mathbf{v}$ on the four triangles by a vector (c_1, c_2, c_3, c_4), we have

$$\left(\operatorname{div} \mathbf{V}_h^{PS}\right)_{Q_h} = \operatorname{Span}\left\{ \begin{pmatrix} 1 \\ 1 \\ 1 \\ 1 \end{pmatrix}, \begin{pmatrix} 1 \\ 1 \\ -1 \\ -1 \end{pmatrix}, \begin{pmatrix} 1 \\ -1 \\ -1 \\ 1 \end{pmatrix} \right\}.$$

In particular, if $\mathbf{v} = \mathbf{v}_1 \in \mathbf{V}_1^{PS}$, i.e., $\mathbf{v}$ is one vector of one linear polynomial on T_1 and T_2, and of another linear polynomial on T_3 and T_4, (to be precise, $\mathbf{v}(P_5) = (c\mathbf{v}(P_1) + \mathbf{v}(P_3))/(c+1)$) then $\operatorname{div} \mathbf{v}|_{T_2} = \operatorname{div} \mathbf{v}|_{T_1}$, and $\operatorname{div} \mathbf{v}|_{T_3} = \operatorname{div} \mathbf{v}|_{T_4}$:

$$\left(\operatorname{div} \mathbf{V}_1^{PS}\right)_{Q_h} = \operatorname{Span}\left\{ \begin{pmatrix} 1 \\ 1 \\ 1 \\ 1 \end{pmatrix}, \begin{pmatrix} 1 \\ 1 \\ -1 \\ -1 \end{pmatrix} \right\}. \tag{3.10}$$

On the other side, for any $\mathbf{v} = \mathbf{v}_2 \in \mathbf{V}_2^{PS}$, $\mathbf{v}(P_i) = \mathbf{0}$ for $i = 1, 2, 3, 4$. That is $\mathbf{v} = \mathbf{v}(P_5)\phi_5$, cf. Fig. 3.6. We have

$$\left(\operatorname{div} \mathbf{V}_2^{PS}\right)_{Q_h} = \operatorname{Span}\left\{ \begin{pmatrix} 1 \\ 1 \\ -1 \\ -1 \end{pmatrix}, \begin{pmatrix} 1 \\ -1 \\ -1 \\ 1 \end{pmatrix} \right\}. \tag{3.11}$$

To decompose $\mathbf{V}_2^{PS}$ further, we write

$$\mathbf{v}_2|_{Q_h} = \mathbf{v}(P_5)\phi_5 = \begin{pmatrix} u_5 \\ v_5 \end{pmatrix} \phi_5 = \mathbf{v}_{2,1} + \mathbf{v}_{2,2}, \tag{3.12}$$

where

$$\mathbf{v}_{2,2} = \mathbf{v}(P_5)\phi_5 - \mathbf{v}_{2,1}, \quad \text{and} \quad \mathbf{v}_{2,1} = \frac{\hat{x}_2 u_5 + \hat{y}_2 v_5}{\sqrt{\hat{x}_2^2 + \hat{y}_2^2}} \begin{pmatrix} \hat{x}_2 \\ \hat{y}_2 \end{pmatrix} \phi_5.$$

It is straightforward to verify that, by (3.9),

$$\begin{cases} \operatorname{div} \mathbf{v}_{2,1} \in \left(\operatorname{div} \mathbf{V}_1^{PS}\right)_{Q_h}, \\ (\operatorname{div} \mathbf{v}_{2,2}, \operatorname{div} \mathbf{v}_1)_{L^2(Q_h)} = 0 \quad \forall \mathbf{v}_1 \in \mathbf{V}_1^{PS}. \end{cases} \tag{3.13}$$

We note that the separation of $\left(\operatorname{div} \mathbf{V}_2^{PS}\right)_{Q_h}$ in (3.13) is done by separating its two basis functions in (3.11) according to the structure of $\left(\operatorname{div} \mathbf{V}_1^{PS}\right)_{Q_h}$ in (3.10). Now (3.8) can be decomposed further as

$$\mathbf{w} = \mathbf{w}_1 + \mathbf{w}_2 = (\mathbf{w}_1 + \mathbf{w}_{2,1}) \oplus (\mathbf{w}_{2,2}) \tag{3.14}$$

such that

$$\operatorname{div}(\mathbf{w}_1 + \mathbf{w}_{2,1}) \in \hat{P}_h, \text{ and } (\operatorname{div} \mathbf{w}_{2,2}, q_h)_{L^2(\Omega)} = 0 \quad \forall q_h \in \hat{P}_h. \tag{3.15}$$

By (3.14), as $q_1 := \operatorname{div}(\mathbf{w}_1 + \mathbf{w}_{2,1}) \in \hat{P}_h$, by Lemma 3.2, there is a $\mathbf{v}_h \in \mathbf{V}_h^{PS}$ such that

$$b(\mathbf{v}_h, q_1) \geq C|\mathbf{v}_h|_{H^1(\Omega)}\|q_1\|_{L^2(\Omega)}. \tag{3.16}$$

Further more, we scale $\mathbf{v}_h$ on both sides of (3.16) so that

$$C|\mathbf{v}_h|_{H^1(\Omega)} = \|q_1\|_{L^2(\Omega)}. \tag{3.17}$$

By the same way as in the decomposition (3.14) and (3.15), we write

$$\mathbf{v}_h = (\mathbf{v}_1 + \mathbf{v}_{2,1}) \oplus (\mathbf{v}_{2,2}), \quad \mathbf{v}_{2,2} \in \mathbf{V}_2^{PS}.$$

It is clear now how to select a $\mathbf{v} \in \mathbf{V}_h^{PS}$ for the given $\mathbf{w}_h$ to satisfy the inf-sup condition (3.4):

$$\mathbf{v} = \mathbf{v}_h + (-\mathbf{w}_{2,2} - \mathbf{v}_{2,2}) = (\mathbf{v}_1 + \mathbf{v}_{2,1}) \oplus (-\mathbf{w}_{2,2}). \tag{3.18}$$

By the L^2-orthogonality in (3.14) and (3.18), it follows that

$$\begin{aligned} b(\mathbf{v}, q_h) &= -(\operatorname{div} \mathbf{v}, q_1) - (\operatorname{div} \mathbf{v}, \operatorname{div} \mathbf{w}_{2,2}) \\ &= -(\operatorname{div}(\mathbf{v}_1 + \mathbf{v}_{2,1}), q_1) + (\operatorname{div} \mathbf{w}_{2,2}, \operatorname{div} \mathbf{w}_{2,2}) \\ &= b(\mathbf{v}_h, q_1) + \|\operatorname{div} \mathbf{w}_{2,2}\|_{L^2(\Omega)}^2. \end{aligned}$$

By the reduced inf-sup condition (3.16) and (3.17), we get further that

$$\begin{aligned} b(\mathbf{v}, q_h) &\geq C|\mathbf{v}_h|_{H^1(\Omega)}\|q_1\|_{L^2(\Omega)} + \|\operatorname{div} \mathbf{w}_{2,2}\|_{L^2(\Omega)}^2 \\ &= \left(C^2|\mathbf{v}_h|_{H^1(\Omega)}^2 + |\operatorname{div} \mathbf{w}_{2,2}|_{L^2(\Omega)}^2\right)^{\frac{1}{2}} \left(\|q_1\|_{L^2(\Omega)}^2 + \|\operatorname{div} \mathbf{w}_{2,2}\|_{L^2(\Omega)}^2\right)^{\frac{1}{2}} \\ &\geq \left(C^2|\mathbf{v}_h|_{H^1(\Omega)}^2 + C_1^2|\mathbf{w}_{2,2}|_{H^1(\Omega)}^2\right)^{\frac{1}{2}} \|q_h\|_{L^2(\Omega)} \\ &\geq \min\{C, C_1\}|\mathbf{v}|_{H^1(\Omega)}\|q_h\|_{L^2(\Omega)}, \end{aligned}$$

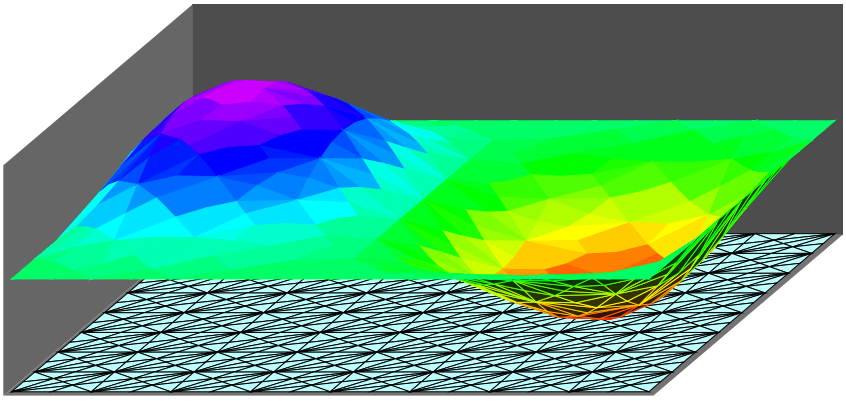

Fig. 4.1. The first component of $\mathbf{u}_h$ on the 4th level grid.

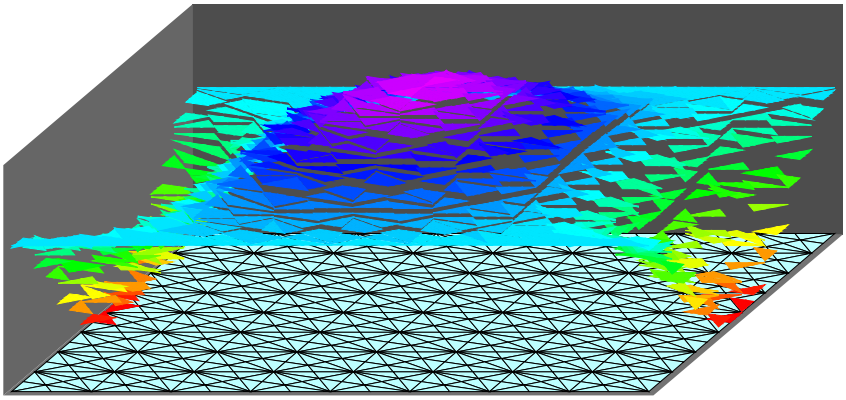

Fig. 4.2. The pressure p_h on the 4th level grid.

where we used an easily verifiable fact $|\mathbf{w}_{2,2}|_{H^1(\Omega)} = \sqrt{2}\|\operatorname{div}\mathbf{w}_{2,2}\|_{L^2(\Omega)}$ for hat functions supported on squares (cf. [12]), which ensures (by an referencing mapping) that

$$|\mathbf{w}_{2,2}|_{H^1(\Omega)} \le C_1^{-1}\|\operatorname{div}\mathbf{w}_{2,2}\|_{L^2(\Omega)}$$

with C_1 independent of h but dependent on the regularity (3.1) of triangulation Ω_h because $\mathbf{w}_{2,2}$ is supported locally on quadrilaterals like the Q_h shown in Fig. 3.6. □

Theorem 3.2. *The Powell-Sabin P_1 divergence-free solution $(\mathbf{u}_h, p_h)$ for the Stokes equations* (2.6) *is of optimal order in approximation:*

$$\|\mathbf{u} - \mathbf{u}_h\|_{H^1} + \|p - p_h\|_{L^2} \le Ch(\|\mathbf{u}\|_{H^2} + \|p\|_{H^1}).$$

Proof. By the inf-sup condition (3.7), the approximation of the mixed-element is quasi-optimal, by the classic mixed finite element theorem [6, 12], namely,

$$\|\mathbf{u} - \mathbf{u}_h\|_{H^1} + \|p - p_h\|_{L^2} \le C \inf_{\mathbf{v}_h \in \mathbf{V}_h^{PS}} \|\mathbf{u} - \mathbf{v}_h\|_{H^1(\Omega)^2} + C \inf_{q_h \in P_h} \|p - q_h\|_{L^2(\Omega)}.$$

Noticing $P_h \supset \hat{P}_h$ defined in (3.5) — the space of 3 piecewise constants on each triangle of $\tilde{\Omega}_h$, the proof is complete. □

Table 4.1: The Powell-Sabin solutions by the iterated penalty method (2.8)-(2.9).

Level	Grid	# triangles	$\lvert\mathbf{u}-\mathbf{u}_h\rvert_{H^1}$	$\lVert p-p_h\rVert_{L^2}$	$\lvert\mathbf{u}-\mathbf{u}_h\rvert_{l_\infty}$	$\lVert p-p_h\rVert_{l_\infty}$
2	2×2	48	2.42444	5.65923	5.65923	9.54726
3	4×4	192	1.31865	2.91791	0.15469	5.51233
4	8×8	768	0.67491	1.44462	0.05398	3.23210
5	16×16	3072	0.33514	0.71194	0.01544	1.72471
6	32×32	12288	0.16663	0.35458	0.00413	0.90545
7	64×64	49152	0.08306	0.17711	0.00107	0.46507

Table 4.2: The P_1 divergence-free element on the uniform grids.

Level	Grid	# triangles	$\lvert\mathbf{u}-\mathbf{u}_h\rvert_{H^1}$	$\lVert p-p_h\rVert_{L^2}$	$\lvert\mathbf{u}-\mathbf{u}_h\rvert_{l_\infty}$	$\lVert p-p_h\rVert_{l_\infty}$
3	4×4	32	3.10367	13.26644	0.75000	16.48328
4	8×8	128	3.52223	31.20645	0.75000	67.44058
5	16×16	512	3.62370	65.30492	0.76172	174.82793
6	32×32	2048	3.63142	130.72432	0.76500	383.22368
7	64×64	8192	3.64096	212.58133	0.76912	728.41291
∞			$\not\to 0$	$\to\infty$	$\not\to 0$	$\to\infty$

4. Numerical Tests

In this section, we report some results of numerical experiments of the P_1 divergence-free element on the uniform cross grids, and on the Powell-Sabin grids, shown in the left graph and the right graph of Fig. 3.2.

The computational domain Ω for (2.6) is the unit square. The unit square is first partitioned into $n\times n$ small squares, then $2(n\times n)$ triangles. The partition is denoted by $\tilde{\Omega}_h$, shown in the left graph of Fig. 3.2. Each triangle of $\tilde{\Omega}_h$ is further subdivided into 6 subtriangles by connecting the center of mass with the three vertices and the three mid-edge points, shown by Ω_h in the right graph of Fig. 3.2. This is a simplified version of Powell-Sabin grids, described in Section 3.

The right hand side function $\mathbf{f}$ for (2.6) is

$$\mathbf{f} = -\Delta\,\mathbf{curl}\, g - \nabla g_{xx} = \begin{pmatrix} -g_{yxx} - g_{yyy} - g_{xxx} \\ g_{xxx} + g_{xyy} - g_{yxx} \end{pmatrix}. \tag{4.1}$$

where $g = 2^8(x-x^2)^2(y-y^2)^2$. The continuous solution for the Stokes equations (2.1) is

$$\mathbf{u} = \mathbf{curl}\, g, \quad p = -g_{xx}. \tag{4.2}$$

We plot the first component of the numerical solution $\mathbf{u}_h$ in Fig. 4.1, and p_h in Fig. 4.2, for $h = 0.125$ (i.e., on the 4-th level grid, see Table 4.1) by the Powell-Sabin P_1 divergence-free method.

In Table 4.1, we list the errors of the Powell-Sabin P_1 divergence-free element on several levels of grids. The order of convergence for the velocity in the H^1-norm and the order for the pressure in the L^2-norm are apparently both 1, verifying the theory presented in Theorem 3.2. Also in Table 4.1, we can see that the nodal error for the velocity converges at order 2, while that for the pressure at order 1, as expected, though not proved in this paper.

In Table 4.2, we list the errors of the P_1 divergence-free element on the uniform grids, shown in the left graph of Fig. 3.2. It is well known that such a conforming P_1 method has a locking

Table 4.3: The inf-sup constant in (3.7) for the Powell-Sabin P_1 element.

Level	Grid	$\dim \mathbf{V}_h^{PS}$	$\dim \mathbf{Z}_h$	inf-sup constant in (3.7)
1	1×1	6	2	0.286344198474493
2	2×2	34	8	0.258961387083094
3	4×4	162	56	0.272567422851668
4	8×8	706	296	0.274357431100380
5	16×16	5892	1352	0.275426941311122

problem. The numerical data in Table 4.2 show that there is no approximation at all for the P_1 divergence-free element on the uniform grids. We can see that the discrete solutions for the velocity go to zero, and that the discrete solutions for the pressure diverge to infinity.

Finally, we verify the inf-sup condition (3.7). The inf-sup constant is equal to the square root of the minimum eigenvalue of matrix $A^{-1}B$, where A and B are the matrices arising from the $a(\cdot,\cdot)$ inner product and the $(\operatorname{div}\cdot, \operatorname{div}\cdot)$ inner product under the nodal basis (or any basis) of $\mathbf{V}_h^{PS}$, respectively. We note that the number of zero eigenvalues is the dimension of divergence-free space $\mathbf{Z}_h$. The computed inf-sup constants on each level of grids are listed in Table 4.3.

References

[1] P. Alfeld and L.L. Schumaker, Smooth macro-elements based on Powell-Sabin triangle splits, *Adv. Comput. Math.*, **16** (2002), 29-6.

[2] D.N. Arnold and J. Qin, Quadratic velocity/linear pressure Stokes elements, in Advances in Computer Methods for Partial Differential Equations VII, ed. R. Vichnevetsky and R.S. Steplemen, 1992.

[3] G. Baker, W. Jureidini and A. Karakashian, Piecewise solenoidal vector fields and the Stokes problem, *SIAM J. Numer. Anal.*, **27** (1990), 1466-1485.

[4] S.C. Brenner, An optimal-order multigrid method for P1 nonconforming finite elements, *Math. Comp.*, **52** (1989), 1-15.

[5] S.C. Brenner and L.R. Scott, The Mathematical Theory of Finite Element Methods, Springer-Verlag, New York, 1994.

[6] F. Brezzi and M. Fortin, Mixed and hybrid finite element methods, Springer, 1991.

[7] J. Carrero, B. Cockburn and D. Schötzau, Hybridized globally divergence-free LDG methods. I. The Stokes problem, *Math. Comput.*, **75** (2006), 533-563.

[8] S.-S. Chow and G.F. Carey, Numerical approximation of generalized Newtonian fluids using Powell-Sabin-Heindl elements: I. theoretical estimates, *Int. J. Numer. Meth. Fl.*, **41** (2003), 1085-1118.

[9] P.G. Ciarlet, The Finite Element Method for Elliptic Problems, North-Holland, Amsterdam, 1978.

[10] B. Cockburn, F. Li and C.-W. Shu, Locally divergence-free discontinuous Galerkin methods for the Maxwell equations, *J. Comput. Phys.*, **194** (2004), 588-610.

[11] M. Fortin and R. Glowinski, Augmented Lagrangian Methods: Applications to the Numerical Solution of Boundary-value Problems, North Holland, Amsterdam, 1983.

[12] V. Girault and P.A. Raviart, Finite element methods for Navier-Stokes equations, Springer, 1986.

[13] H. Juarez, L.R. Scott, R. Metcalfe, and B. Bagheri, Direct simulation of freely rotating cylinders in viscous flows by high-order finite element methods, *Comput. & Fluids*, **29** (2000), 547-582.

[14] O. Karakashian and T. Katsaounis, Numerical simulation of incompressible fluid flow using locally solenoidal elements, *Comput. Math. Appl.*, **51** (2006), 1551-1570.
[15] M.-J. Lai and L.L. Schumaker, Macro-elements and stable local bases for splines on Powell-Sabin triangulations, *Math. Comput.*, **72** (2001), 335-354.
[16] M.J. Lai and L.L. Schumaker, Macro-elements and stable local bases for splines on Clough-Tocher triangulations, *Numer. Math.*, **88** (2001), 105-119.
[17] F. Li and C.-W. Shu, Locally divergence-free discontinuous Galerkin methods for MHD equations, *J. Sci. Comput.*, **22/23** (2005), 413-442.
[18] J.-C. Nédélec, Éléments finis mixtes incompressibles pour l'équation de Stokes dans R3, *Numer. Math.*, **39** (1982), 97-112.
[19] G. Nürnberger and F. Zeilfelder, Developments in bivariate spline interpolation, *J. Comput. Appl. Math.*, **121** (2000), 125-152.
[20] P. Oswald, Hierarchical conforming finite element methods for the biharmonic equation, *SIAM J. Numer. Anal.*, **29** (1992), 1610-1625.
[21] P. Oswald, Remarks on multilevel bases for divergence-free finite elements, *Numer. Algorithms*, **27** (2001), 131-152.
[22] M.J.D. Powell, Piecewise quadratic surface fitting for contour plotting, in Software for Numerical Mathematics, ed. D. J. Evans, Academic Press, New York, 1976, 253-2271.
[23] M.J.D. Powell and M.A. Sabin, Piecewise quadratic approximations on triangles, *ACM Math.Software*, **3/4** (1977), 316-25.
[24] J. Qin , On the convergence of some low order mixed finite elements for incompressible fluids, Thesis, Pennsylvania State University, 1994.
[25] J. Qin and S. Zhang, Stability and approximability of the P1-P0 element for Stokes equations, *Int. J. Numer. Meth. Fl.*, **54** (2007), 497-515.
[26] L.L. Schumaker, On super splines and finite elements, *SIAM J. Numer. Anal.*, **26** (1989), 997-1005.
[27] L.L. Schumaker and T. Sorokina, Smooth macro-elements on Powell-Sabin-12 splits, *Math. Comput.*, **75** (2005), 711-726.
[28] L.R. Scott and M. Vogelius, Norm estimates for a maximal right inverse of the divergence operator in spaces of piecewise polynomials, *RAIRO, Modelisation Math. Anal. Numer.*, **19** (1985), 111-143.
[29] L. R. Scott and M. Vogelius, Conforming finite element methods for incompressible and nearly incompressible continua, in Lectures in Applied Mathematics, **22** (1985), 221-244.
[30] L. R. Scott and S. Zhang, Multilevel Iterated Penalty Method for Mixed Elements, the Proceedings for the Ninth International Conference on Domain Decomposition Methods, 133-139, Bergen, 1998.
[31] R. Stenberg, Analysis of mixed finite element methods for the Stokes problem: a unified approach, *Math. Comput.*, **42** (1984), 9-23.
[32] X. Ye and G. Anderson, The derivation of minimal support basis functions for the discrete divergence operator, *J. Comput. Appl. Math.*, **61** (1995), 105-116.
[33] X. Ye and C. A. Hall, A discrete divergence-free basis for finite element methods, *Numer. Algorithms*, **16** (1997), 365-380.
[34] S. Zhang, A new family of stable mixed finite elements for 3D Stokes equations, *Math. Comput.*, **74**:250 (2005), 543-554.
[35] S. Zhang, A C1-P2 finite element without nodal basis, *M2AN*, **42** (2008), 175-192.